Hindawi
Mobile Information Systems
Volume 2022, Article ID 4284734, 8 pages
https://doi.org/10.1155/2022/4284734

Research Article

Application of Robust Data Link Optimization in Medical Protein Nutrition Intervention Based on Ensemble Learning Algorithms

Xiaowen Hou

School of Economics and Management, Beijing Information Technology College, Beijing, China

Correspondence should be addressed to Xiaowen Hou; houxw@bitc.edu.cn

Received 24 May 2022; Revised 21 June 2022; Accepted 5 July 2022; Published 20 July 2022

Academic Editor: Shadi Aljawarneh

Research on 6G-related technologies based on the Internet of Things (IoT) has attracted widespread attention from research units, universities, and industry, and there are still some important issues that need to be resolved urgently. How to ensure robust data link optimization for data transmission in a band-limited nonstationary environment at a lower cost is a very important issue. Based on the current research status of specific medical protein POCT products at home and abroad, this paper has designed and developed a specific medical protein detection system with simple operation, rapid detection, and small volume: according to the Lambert Beer's law, we adopt the transmission colorimetry method (transmittance Turbidity method), with the optical part, electronic part, and mechanical part as the structure, carry out the design work of optoelectronics and software. It also evaluates the serum nutritional indicators and gastrointestinal function of abdominal surgery patients after nutritional intervention combined with emotional nursing and expands the reference basis for intervention methods for abdominal surgery patients. Using this experimental method, after the samples are selected by the CART algorithm, the accuracy of the running results is higher.

1. Introduction

By collecting large amounts of mobile data and analyzing voice data mining, the wireless network can be optimized and the quality of the mobile communication network can be improved. Wireless network optimization refers to the reasonable allocation of the production network and formal investment of resources mainly through the collection of parameters and analysis of data, and reasonable optimization of the network operation status [1]. It is to find out the quality problems in the network operation process and use parameter settings to solve network quality problems. And, put forward reasonable network maintenance and find out various optimization methods for planning and construction plans. Based on the research of related theories about the application of voice data mining technology in mobile communication networks, find out a suitable data analysis method for mobile communication networks. This article introduces a low-complexity, low-power modulation, and demodulation transmission technology, namely, differential chaotic keying (DCSK) modulation [2]. And, this paper, respectively, describes and analyzes the robust data link optimization, advantages, and improvement methods of the system in standard and nonstandard transmission environments. At the same time, some new coding and modulation schemes based on multiple DCSK (MDCSK) will be provided to improve the transmission quality of the system in a band-limited environment, which will help in low-power, low-cost networks, especially on nonstationary channels. the robust data link optimization of the system is improved [3]. The results show that these optimization works have significantly improved the system performance. Afterwards, the optimization of system parameters for nonstationary channel characteristics and the adaptive transmission mechanism will become the focus of future research. The specific medical protein analyzer is a device that checks the level of specific immune proteins in serum, plasma, or urine to determine their content accurately and effectively to assist doctors in clinical diagnosis [4]. During the operation of the instrument, professional medical

personnel first collect, identify, process, and store the samples, separate the active ingredients from the samples to be tested obtained from the test objects, and mark all samples corresponding to their test objects [5]. At present, the most common test items of specific medical protein analyzers mainly include the detection of myocardial protein markers (myoglobin, etc.) and the detection of nephropathy protein markers [6]. The combination of nutritional intervention and emotional care can improve the nutritional status of diabetic patients. Patients undergoing abdominal surgery can enhance immune function, promote the recovery of gastrointestinal function, and reduce postoperative complications. In addition, the control group received routine nutrition interventions, such as health education, psychological care, primary care, and prevention of complications, and the observation group received a combination of early nutrition intervention and emotional care to realize the application of medical protein nutrition intervention [7].

2. Related Work

The literature introduces a large-scale automatic protein detection instrument with high throughput, automation, and high speed, which requires professional operation training and is operated by professional medical personnel [8]. The reagents and samples are processed before use and the detection can be performed automatically. Multichannel multisample detection can be processed at one time. Hospitals above Grade A and large testing institutions have a large number of people to test each day, and the testing needs are large. The automatic analyzer can automatically perform testing, and perform result judgment, and report printing, which reduces time and human resources, and satisfies the testing well [9]. The literature introduces the rapid and convenient POCT rapid detection. The outpatient volume of grassroots hospitals is small, and the samples are correspondingly small. The use and maintenance cost of high-throughput specific immune protein detection equipment is high, which is bound to cause waste. Therefore, a POCT type rapid tester should be selected in such facilities [10]. This type of product is also suitable for outpatient laboratories, emergency rooms, rapid test centers, municipal hospitals, etc. The literature introduces the importance of theoretical research on the classification of differentiated image data with several samples and the classification of speech data with one sample and emphasizes their application in high-throughput light screening and language-independent speech recognition, it depends on the angle of the speaker application [11]. By analyzing the problems in the existing image and audio data classification methods, the most important research content in this article can be determined. The literature describes the classification of cytoplasmic images [12]. Taking the information distance theory as a reference, the MPEG compression algorithm is used to rewrite the information distance equation, and according to the application characteristics of MPEG, the similarity between cytoplasmic images is evaluated [13]. Experimental results show that this method is similar to the results of traditional analysis methods. Because the cost of biological experiments is high, the data set used does not need to be verified for the second time by biological experiments, so it is impossible to compare the profit indicators of this method. The literature introduces a dynamic time warping algorithm for combining weights [14]. The attributes of speech data are analyzed, combined with the dynamic time warping algorithm, the reliability index is defined, and a new weighted dynamic time warping algorithm is proposed, which can be used for speech recognition in silent environments [15]. It can be seen from the results that this method can improve the recognition speed without affecting the accuracy of speech recognition.

3. Theoretical Basis of Voice Data Mining and Robust Data Link Optimization

3.1. Speech Data Mining Algorithm Design. The PD audio data samples contain 26 samples, which correspond to audio segments of 26 individuals. Due to the difference in the range and tone of each person's voice, some samples cannot describe the essential difference between PD patients and healthy people. Finding the most valuable samples in the right way is of great benefit to research. This article recommends using the CART algorithm to select samples.

Through the prior knowledge of the pathologist, the features in the PD data are extracted, which contains a total of 26 features. There is a big gap between feature values because different features have different physical meanings and calculation methods. Many machine learning algorithms are sensitive to the number of feature values. To solve this problem, this article uses a normalization method to normalize all functions to actual values between 0 and 1. Assuming that the training set is represented by X, the test set is represented by T, $x\_\max$ represents the largest vector of features, and x_min represents the smallest vector of features, then

$$X\prime = \frac{(X - x\_\min)}{x\_\max - x\_\min}, \tag{1}$$

$$T'\frac{(T - x\_\min)}{x\_\max - x\_\min}. \tag{2}$$

M classification task, P_m is the probability that the sample belongs to the m-th category, then the Gini coefficient of this probability distribution is defined as follows:

$$\mathrm{Gini}(p) = \sum_{m=1}^{M} p_m(1 - p_m) = 1 - \sum_{m=1}^{M} p_m^2. \tag{3}$$

For the binary classification problem, assuming that the probability of the first sample type is p, then the Gini coefficient of the probability distribution is

$$\mathrm{Gini}(p) = 2p(1 - p). \tag{4}$$

Given two types of sample sets D Gini index is defined as follows:

$$\text{Gini}(D) = 1 - \sum_{m=1}^{2}\left(\frac{|C_m|}{|D|}\right)^2. \tag{5}$$

$$\text{Gini}(D,T) = \frac{|D_1|}{|D|}\text{Gini}(D_1) + \frac{|D_2|}{|D|}\text{Gini}(D_2). \tag{6}$$

If CART is "too deep," overfitting will occur. In other words, the performance on the training set is very good, but the performance on the test set is very poor. Currently, pruning is a good way to do this. The cleaning algorithm is divided into two steps: first, get many subtrees, starting from the bottom of the entire spanning tree, and then continue cutting to the CART root node. The second is to choose the best subtree and use a different set of validations to cross-validate all subtrees and obtain the best structure. This operation can be performed when the amount of data is sufficient, but it is difficult to process medical data due to the small amount of medical data and the high cost of obtaining new samples. Therefore, this article uses another method to control the overfitting of CART. When generating CART, the minimum number of leaf node samples will be specified. This can effectively control the depth of the tree, so as to obtain the best effect on the model.

The Pearson correlation coefficient is usually used to measure the linear correlation between feature f and category C, as shown in the following equation:

$$R(i) = \frac{\text{cov}(X_i, Y)}{\sqrt{\text{var}(X_i)\text{var}(Y)}}. \tag{7}$$

The intraclass distance is the square of the distance between each sample in the same class. The distribution of the sample points around the mean is reflected by the within-class variance, and the formula is as follows:

$$d^2(w_i) = \frac{1}{N_i}\sum_{k=1}^{N_i}\left(\mathrm{x}_{i,k} - \mathrm{m}_i\right)^T\left(\mathrm{x}_{i,k} - \mathrm{m}_i\right), \tag{8}$$

$$S_{w_i} = \frac{1}{N_i}\sum_{k=1}^{N_i}\left(x_{i,k} - m_i\right)\left(x_{i,k} - m_i\right)^T. \tag{9}$$

The intraclass distance and intraclass scatter matrix are transformed into rank relations,

$$d^2(w_i) = Trr\left[S_{w_i}\right]. \tag{10}$$

The relationship between the intraclass, interclass, and total allocation matrix in multiclass situations,

$$S_w = \sum_{i=1}^{c} P_i S_{w_i} = \sum_{i=1}^{c} P_i \frac{1}{N_i}\sum_{k=1}^{N_i}\left(x_{i,k} - m_i\right)\left(x_{i,k} - m_i\right)^T. \tag{11}$$

The total between-class deviation matrix,

$$S_B = \sum_{i=1}^{c} P_i\left(m_i - m\right)\left(m_i - m\right)^T. \tag{12}$$

Overall scatter matrix,

$$S_T = \frac{1}{N}\sum_{l=1}^{N}\left(x_l - m\right)\left(x_l - m\right)^T = S_W + S_B, \tag{13}$$

$$d^2(\vec{x}) = Tr\left[S_w + S_B\right] = Tr\left[S_T\right]. \tag{14}$$

When deriving and actually applying certain relationships, the following statistics can replace them.

$$P_i = \frac{N_i}{N}, m_i = \frac{1}{N_i}\sum_{k=1}^{N_i}\vec{x}_k^{(i)}, m = \frac{1}{N}\sum_{l=1}^{N}\vec{x}_l. \tag{15}$$

Assuming that there are m neurons in the visual layer of RBM and n neurons in the hidden layer, the energy function of the neurons in the i-th visual layer is shown as follows:

$$E(V,H|\theta) = -\sum_{i=1}^{m} a_i v_i - \sum_{j=1}^{n} b_j h_j - \sum_{i=1}^{m}\sum_{j=1}^{n}\omega_{ij} v_i h_j. \tag{16}$$

The joint probability distribution of (V,H) is

$$P(V,H|\theta) = \frac{e^{-E(v,H\theta)}}{A(\theta)}, A(\theta) = \sum_{v,H} e^{-E(v,HH)}. \tag{17}$$

The observation of the data distribution V is the key point. It is the probability function of the common probability distribution $P(V, H|\theta)$ of the input data.

$$P(V|\theta) = \frac{1}{A(\theta)}\sum_{y} e^{-E(V,H|\theta)}. \tag{18}$$

RBM is an asymmetric structure. The activation probability of each neuron is conditionally independent of each other. The activation probabilities of the i-th unit in the visible layer and the j-th unit in the hidden layer are calculated separately.

$$P\left(v_i = 1|H,\theta\right) = \sigma\left(a_i + \sum_j \omega_{ij} h_j\right). \tag{19}$$

$$P\left(h_j = 1H,\theta\right) = \sigma\left(b_j + \sum_i v_i \omega_{ij}\right). \tag{20}$$

The integrated learning algorithm consists of two parts optimized based on the CART example. The first is to use the CART algorithm to select the best sample. The second is to combine the results of the RF, SVM, and ELM classifiers to perform joint decisions. In this section, LOO and LOSO will be used to organize experiments. It can be seen from the experimental results that LOSO can effectively overcome the differences in audio samples, is usually more effective than LOO, and mainly involves the final prediction of the object. We do not make requirements for the actual prediction of a single sample, so this section mainly uses experimental LOSO results to test performance.

Integrate three algorithms RF, SVM, and ELM to predict the test set. Using the Gini coefficient of the spanning tree model, RF contains 500 CARTs. After CART optimization, samples and features are randomly selected from the sample

Table 1: Integrated learning classification results under LOO.

Classification algorithm		LOO (%)		
		Correct rate	Sensitivity	Specificity
RF_with CART	Mean	70.80	72.20	69.50
	Best value	71.40	72.90	70.40
SVM(linear)_with CART	Mean	65.10	64.40	65.80
	Best value	65.10	64.40	65.80
SVM(rbf)_with CART	Mean	70.19	72.31	68.08
	Best value	70.19	72.31	68.08
ELM_with CART	Mean	60.13	62.44	57.83
	Best value	61.50	63.70	60.40
PD-EL_with CART	Mean	74.50	76.90	72.00
	Best value	75.50	78.30	73.30

set to ensure the diversity of the tree model and improve the stability of the model. For SVM, we use a linear kernel function and a radial basis kernel function. The radial core function solves the problem of linear separability in the source sample space by mapping the data set from the source space to the feature space and mapping the low-dimensional to the high-dimensional. The parameter g is used to control the degree of mapping. These two parameters control the generalization ability of the model. The smaller the parameter value, the higher the accuracy. In the algorithm of this work, the values of C and g are between 1 and 20. In the experiments in this chapter, setting C to 10 and g to 2 is the most effective. ELM is a single hidden layer feedforward neural network with powerful custom functions, but it is more sensitive to parameter selection. ELM training does not require backpropagation, so the calculation is faster and more common, but the results may vary greatly. By integrating multiple classifier models suggested in this chapter, we can effectively reduce variance and increase model stability.

3.2. Analysis of Results. After optimizing the CART example, use the new example set to train RF, SVM, and ELM models. A total of 4 result sets will be obtained. RF_withCART refers to an RF model trained with a new set of samples. SVM (linear)_withCART refers to the new linear kernel SVM training sample set. SVM(rbf)_withCART refers to the radial basis kernel SVM that has been trained using new example sentences. ELM_withCART refers to the ELM model trained with new example sentences. Table 1 lists the classification results of each model.

Compare the PD-EL_withCART algorithm to illustrate the effectiveness and superiority of the algorithm. So far, only four studies of Sakar et al.'s data have been tested, two of which show the classification accuracy of the validation set. It can be seen from the results that no matter how LOO or LOSO changes, the PD-EL_withCART algorithm achieves

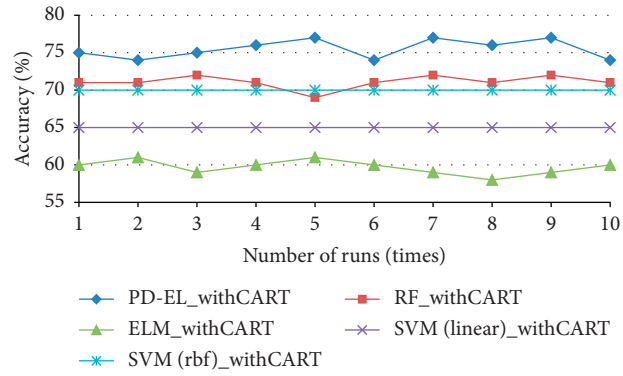

Figure 1: Correction rate curve under LOO.

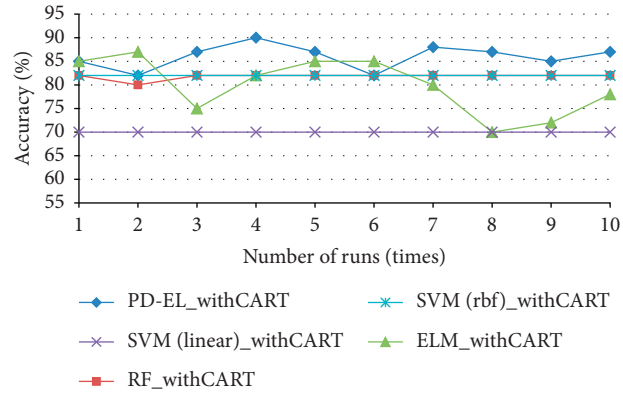

Figure 2: Correction rate curve under LOSO.

Table 2: Classification results of unoptimized samples under LOO.

Classification algorithm		LOO (%)		
		Correct rate	Sensitivity	Specificity
SVM no CART	Average	64.50	65.80	63.30
	The best	64.50	65.80	63.30
RF no CART	Average	67.39	71.65	62.36
	The best	68.46	76.92	60.00
ELM_no CART	Average	61.60	64.00	59.10
	The best	63.30	66.00	62.10
PD-EL_no CART	Average	72.40	74.80	70.00
	The best	73.80	76.20	71.50

the best classification performance in terms of classification accuracy, sensitivity, and specificity. At the same time, because LOSO effectively reduces the differences between volunteer samples, LOSO has better classification performance than LOO.

In order to conduct in-depth research on the classification performance and stability of the ensemble learning algorithm, we ran each algorithm ten times and calculated the correct rate curves for these five algorithms, as shown in Figure 1. The experimental results show that the PD-EL_withCART algorithm has the highest classification accuracy and sensitivity. However, the best stability is the RF_withCART algorithm.

Table 3: Compares the results of the integrated classification algorithm before and after sample selection.

Difference		L00 (%)			LOSO (%)		
		Accuracy	Flexibility	Specificity	Accuracy	Flexibility	Specificity
PD- EL_noCART	Average	72.40	74.80	70.00	83.50	90.00	77.00
	The best	73.80	76.20	71.50	87.50	95.00	80.00
PD-EL_with CART	Average	74.40	76.90	72.00	86.50	95.00	78.00
	The best	75.50	78.30	73.30	90.00	100.00	80.00

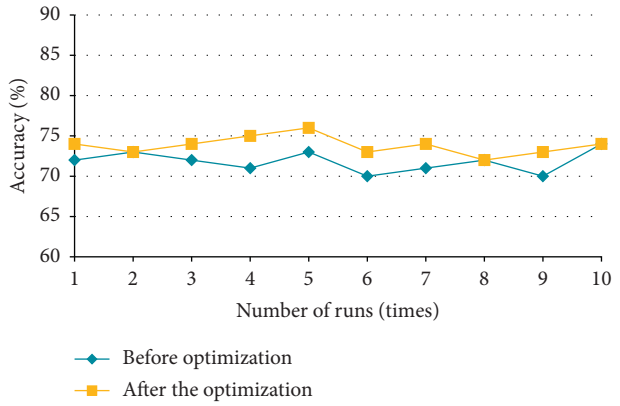

Figure 3: The accuracy curve of the integrated algorithm before and after sample optimization under LOO.

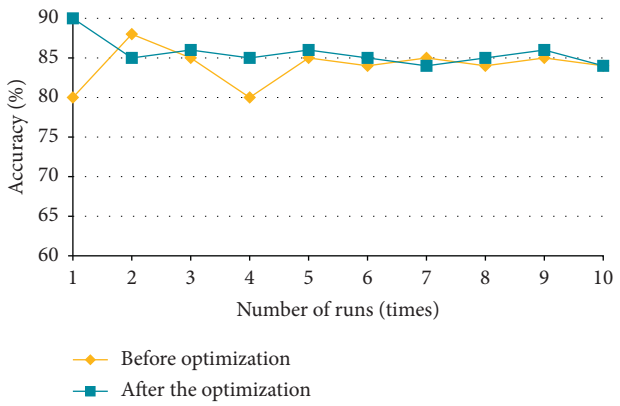

Figure 4: Accuracy curve of the integrated algorithm before and after sample optimization under LOSO.

As shown in Figure 2, the effectiveness of the integrated algorithm is proved by comparing the classification of each classification algorithm in the original data set with the situation after optimizing the CART sample.

As shown in Table 2, without optimizing the CART samples, the overall performance of PD-EL_noCART in this article is the best, with an average accuracy of 83.5%, which is higher than all single classifiers. It can be seen that the ELM algorithm is very sensitive to the initial parameters, and the results of each cycle are very different. Therefore, the ensemble model is suitable for classifying PD samples.

As shown in Table 3, the average accuracy of PD-EL_withCART in LOSO is increased by 3%, the average flexibility is increased by 5%, and the average specificity is increased by 1%, which is the same as the result of the LOO method.

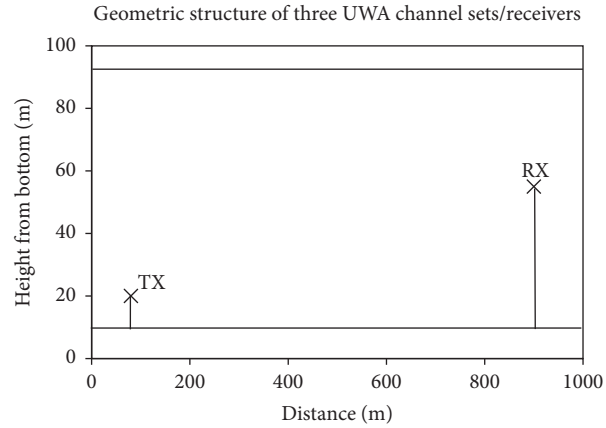

Figure 5: Geometric structure of three UWA channel sets/receivers.

Figure 3 shows the accuracy of the results of 10 executions of LOO and LOSO. Using these two experimental methods, after selecting samples through the CART algorithm, the accuracy of the results of 10 runs is usually the accuracy of the unoptimized sample set.

After optimizing the sample in LOSO, the variance of the accuracy of the 10 results is 0.016, and the variance without optimization is 0.024. After optimizing the sample, you can see that the results are clustered near the mean as shown in Figure 4.

3.3. System Robust Data Link Optimization Design Analysis. Mainly introduces several MDCSK (circular square) signal designs and corresponding coding and modulation systems based on low-cost and low-power consumption under nonstandard channel environment in 6G, respectively, which are optimized for specific nonstationary channel environments. And, the future development direction is given. First, the MDCSK system model used in this system is introduced. Secondly, the optimization of the system itself and the related research work of coding and modulation based on MDCSK are introduced. Then, through examples to demonstrate the constellation based on the MDCSK system and the related modulation and coding structure, code pattern, and related algorithm design and optimization, it can significantly improve the system performance without expanding the bandwidth and achieve low-power consumption. This provides some ideas for the optimal design of the MDCSK data link under nonstationary channels and provides examples of application solutions in specific nonstationary environments, providing the possibility of

Table 4: Comparison of turbidimetric method and turbidimetric method.

Detection method	Scope of test	Detection accuracy	Stability requirements	Reagent price	Calculation method
Turbidimetry	Larger	General	High	General	Simple
Nephelometry	Low concentration	Low concentration and higher	General	High	Complex

Table 5: The protein and calories contained in various foods are as follows.

Category	Weight per serving (g)	Calories (kcal)	Protein (g)
Cereals	25	90	2.0
Vegetables	500	90	5.0
Fruits	200	90	1.0
Soy	25	90	9.0
Milk	160	90	5.0
Meat and eggs	50	90	9.0
Hard fruit	15	90	4.0
Grease	10	90	—

low-cost and low-power implementation in other existing environments. The receiving end obtains the transmission information by directly correlating the signals in the t1 and t2 time periods without channel estimation. The specific positive and negative signals can be expressed as follows:

$$s_1(t) = \begin{cases} +c(t), & 0 \le t < \left(\frac{T}{2}\right), \\ +c\left(t - \left(\frac{T}{2}\right)\right), & \left(\frac{T}{2}\right) \le t < T, \end{cases} \tag{21}$$

$$s_2(t) = \begin{cases} +c(t), & 0 \le t < \left(\frac{T}{2}\right), \\ -c\left(t - \left(\frac{T}{2}\right)\right), & \left(\frac{T}{2}\right) \le t < T. \end{cases} \tag{22}$$

This modulation method has the characteristics of simple equipment and robustness under multipath fading channels, and the corresponding transmission rate decreases accordingly. In order to make the simulation more convincing, the simulation results of 1500 time-varying channel impulse response convolutions are obtained, among which there are channel scenes shown in Figure 5.

Through the performance analysis and research of DCSK in the PLC and UWA environment, it can be seen that because this modulation method does not require the advantages of channel estimation and equalization, it has excellent robustness under nonstationary channels, which is undoubtedly difficult to track and estimate at present.

4. Nutritional Intervention and Application of Medical Protein

4.1. Medical Protein Detection Algorithm Design. In the detection of specific immune proteins, some types of antigens and antibodies specifically bind to form a turbid solution. For example, the NGAL and Cystatin C items detected by this system are not applicable to Lambert Beer's law. It is necessary to select an analytical method for the determination of the concentration of turbidity solution-photoelectric turbidimetry. The photoelectric turbidimetric method is a method of qualitative and quantitative analysis by measuring the degree of turbidity of the solution. It is one of the commonly used medical methods in the detection of specific immune proteins. It has a history of more than 100 years and has played a very important role in many fields. Important role. It has advantages such as cost reduction, ease of use, and high sensitivity. The principle is that as long as the intensity of the incident light is constant, the change of the beam energy conforms to the law of conservation of energy. Because it is difficult to directly measure the intensity of light absorbed in the solution, the intensity of transmitted or scattered light is usually measured to achieve the purpose of quantitative analysis of protein content. The propagation path of light when passing through the turbidity solution can be divided into the transmittance turbidity method.

The calculation formula of the transmittance turbidity method is

$$I_t = I_0 e^{-(\alpha+s)l}. \tag{23}$$

The absorbance value of the suspension to be tested is defined as A, and the absorbance value can also indicate the concentration of the suspension to be tested.

$$A = \lg\left(\frac{I_0}{I_t}\right) = \ln(\alpha + s)l. \tag{24}$$

During the detection process, a beam of incident light with a specific wavelength of Io emitted by the light source passes through the reaction cup containing the suspension to be tested. At this time, equation (24) is derived as follows:

$$A = \lg\left(\frac{V_0}{V_t}\right). \tag{25}$$

Since the relationship between the ratio of incident light to transmitted light and the absorptance is a numerical relationship, the light source, photodetector, and photoelectric processing module in actual sample detection are more stable. When the concentration of the suspension to be tested is low, its absorbance value is correspondingly smaller. If the light source and photovoltaic cell are unstable and the voltage value fluctuates, the absorbance value will fluctuate exponentially. Therefore, this method puts forward higher requirements on the design of the constant current source of the light source and the effect of the photoelectric processing module.

The two turbidimetric detection methods are briefly introduced previosly. Table 4 compares the advantages and disadvantages of the two turbidimetric methods.

Table 6: Comparison of nutritional status between the two groups before and after intervention ($x \pm s$).

Group	n	BM I(kg/m^2)	Hb (g/L)	TP (g/L)	ALB (g/L)	TC (mmol/L)	TG (mmol/L)
Intervention group							
Before intervention	40	17.87 ± 3.32	89.32 ± 8.13	65.19 ± 8.12	36.86 ± 7.30	3.18 ± 0.54	1.25 ± 0.49
After the intervention	40	20.10 ± 4.08 *	97.56 ± 9.45*	70.07 ± 9.87*	41.84 ± 6.43*	4.14 ± 0.43 #	1.68 ± 0.51*
Control group							
Before intervention	40	18.08 ± 3.76	87.89 ± 8.07	67.21 ± 8.43	35.05 ± 5.98	3.21 ± 0.64	1.23 ± 0.46
After the intervention	40	18.57 ± 3.95	90.11 ± 9.85	67.42 ± 9.13	36.13 ± 7.09	3.25 ± 0.49	1.27 ± 0.45

The test method for the NGAL and Cystatin C items detected by the turbidimetric method adopts the two-point endpoint method, and the absorbance calculation refers to the equations (23) and (24) in the calculation of the colorimetric method, which can be obtained by the following equation:

$$\Delta A = A_{R2} - A_{R1}. \tag{26}$$

And, combined with formula (25) for derivation, the final calculation formula of the photoelectric turbidity method of this system is shown in the following equation:

$$A = \frac{5\left(\lg\left(V_0/V_{R2}\right) - \lg\left(V_0/V_{R1}\right)\right)}{3}. \tag{27}$$

4.2. Research Methods of Nutrition Intervention. This group consisted of 80 hemodialysis patients, who were randomly divided into intervention group and control group, with 40 cases in each group. Provide regular health education, and the nurse on duty explains to the patient how to enter the room and the dietary precautions to be taken. When the health education information is updated, the nurse will contact the patient in time and notify the request.

The specific content is sufficient protein and calorie intake: choose high-quality animal protein and instruct patients to perform hemodialysis twice a week. Protein intake should be 1.0–1.2 g per day; limit the intake of egg yolk 3 times a week; eat less seafood and offal. Need to consume a certain amount of calories, maintain a healthy body condition, and determine the daily protein and calorie intake according to the ideal body weight. Ideal weight: standard weight (kg) = [height (cm) − 100] × 0.9, protein intake: total protein (g) = protein intake per kilogram of standard weight × standard weight (kg); total calories (kcal) = Calorie intake per kilogram of standard body weight × standard body weight (kg), to understand the protein and calories required. Drinking water management: daily total fluid intake is limited to 1000 ml. If the urine output is 500 ml/d or more, then the daily water intake (ml) = daily urine output + 500 ml of water, and drink with a solid scale water cup. Daily weight gain should be kept within 1 kg. Sodium salt management: the intake of sodium salt is 3–4 g/day, and the water content is 1000 ml/day. The other is to add 1–2 g/d of salt. You can use vinegar, shallots, garlic, sugar, chili, mustard, etc., instead of salt to increase appetite. Potassium intake management: instruct people who have dialysis twice a week to control their potassium intake to 1.3 g/d. Boil the vegetables in boiling water or cook for 3 minutes before frying. Bibimbap in broth, low-salt, and unsalted soy sauce are prohibited. Frozen food at extremely low temperatures contains 1/3 less potassium than fresh food.

Based on the control group, a nutritional intervention model was established. As the person in charge of health education, nurses regularly and specifically explain how to improve diet and provide adequate nutrition for patients and their families. At the same time, the "24-Hour Diet Review Questionnaire" describes the purpose and method of filling in the form and regularly collects the form to promote patients to strictly abide by the nutritional intervention standards, and timely feedback and diet changes provide information about the nutritional composition. According to Table 5, arrange the required food.

4.3. Research Results of Nutrition Intervention. Generally, the BMI index is a comprehensive index used to assess a person's nutritional status. The BMI index decreases with weight loss, indicating that the body is malnourished. The mild malnutrition of hemodialysis patients reaches 33%, and the severe malnutrition reaches 6%–8%. Among the biochemical indicators, HP, ALB, and blood lipids are important indicators for evaluating nutritional status. The results are shown in Table 6 for a comparison of nutritional status between the two groups before and after the intervention.

4.4. Discussion and Analysis of Medical Protein Nutrition Intervention. The nutritional status of hemodialysis patients is closely related to the occurrence of clinical complications. Although dialysis is widely used, diet management plays an important role in improving the quality of life of patients with chronic renal failure. The incidence of malnutrition in hemodialysis patients is high. Research clearly shows that an insufficient protein energy diet is an important indicator of predicting patient mortality. In this study, the patient's dietary protein, water, potassium, sodium, phosphorus, and other indicators were extensively adjusted to improve the patient's nutritional status.

Drink water from a water cup with identifiable capacity, and every measurement plays a role in strict weight control. Through written teaching methods, patients and their families are taught to effectively manage potassium intake. By repeatedly explaining the diet, chewing calcium and phosphorus adsorbents and taking calcium and phosphorus adsorbents and phosphorus-containing foods at the same time can reduce blood phosphorus and increase blood calcium, supervise the intervention group of patients to learn a scientific and reasonable lifestyle.

5. Conclusion

Generally, the BMI index is a comprehensive index used to assess a person's nutritional status. The BMI index decreases with weight loss, indicating that the body is malnourished. Among the biochemical indicators, HP, ALB, and blood lipids are important indicators for evaluating nutritional status. The accumulation of various toxins in patients with end-stage renal disease can cause gastrointestinal symptoms, loss of appetite, and insufficient protein and calorie intake. A small amount of amino acids and protein are lost during hemodialysis. Some studies believe that ALB is the most valuable indicator for predicting the long-term survival of patients. Anemia in dialysis patients is a relatively common phenomenon. Therefore, evaluating anemia status is the basis for improving the nutritional status of patients. Studies have shown that effective nutritional interventions for hemodialysis patients can significantly increase their energy requirements. Properly regulating the nutritional status by combining the patient's diet and nutrition is very important for the improvement of the patient's survival rate and quality of life.

Data Availability

The data used to support the findings of this study are available from the author upon request.

Conflicts of Interest

The author declares that there are no conflicts of interest.

References

[1] D. Mohammed, M. Omar, and V. Nguyen, "Wireless sensor network security: approaches to detecting and avoiding wormhole attacks," *Journal of Research in Business, Economics and Management*, vol. 10, no. 2, pp. 1860–1864, 2018.

[2] W. M. Tam, F. C. M. Lau, and C. K. Tse, *Digital Communication with Chaos Multiple Access Techniques and Performance*, Elsevier Science, Amsterdam, The Netherlands, 2006.

[3] D. M. Rocke, "Robust control charts," *Technometrics*, vol. 31, no. 2, pp. 173–184, 1989.

[4] T. Nepusz, H. Yu, and A. Paccanaro, "Detecting overlapping protein complexes in protein-protein interaction networks," *Nature Methods*, vol. 9, no. 5, pp. 471-472, 2012.

[5] H. N. Chua, K. Ning, W. K. Sung, H. W. Leong, and L. Wong, "Using indirect protein-protein interactions for protein complex prediction," *Journal of Bioinformatics and Computational Biology*, vol. 06, no. 03, pp. 435–466, 2008.

[6] B. Xu, H. Lin, and Z. Yang, "Ontology integration to identify protein complex in protein interaction networks," *Proteome Science*, vol. 9, no. 1, p. S7, 2011.

[7] X. Tang, J. Wang, and Y. Pan, "Predicting protein complexes via the integration of multiple biological information," in *Proceedings of the 2012 IEEE 6th International Conference on Systems Biology*, pp. 174–179, IEEE, Xi'an, China, August 2012.

[8] X. Lei, F. Wang, F.-X. Wu, A. Zhang, and W. Pedrycz, "Protein complex identification through Markov clustering with firefly algorithm on dynamic protein-protein interaction networks," *Information Sciences*, vol. 329, pp. 303–316, 2016.

[9] Y. J. Zhang, H. F. Lin, Z. Yang, and J. Wang, "Construction of dynamic probabilistic protein interaction networks for protein complex identification," *BMC Bioinformatics*, vol. 17, no. 1, p. 186, 2016.

[10] L. Ou-Yang, D. Q. Dai, X. L. Li, M. Wu, X. F. Zhang, and P. Yang, "Detecting temporal protein complexes from dynamic protein-protein interaction networks," *BMC Bioinformatics*, vol. 15, no. 1, p. 335, 2014.

[11] B. Futcher, G. I. Latter, P. Monardo, C. S. McLaughlin, and J. I. Garrels, "A sampling of the yeast proteome," *Molecular and Cellular Biology*, vol. 19, no. 11, pp. 7357–7368, 1999.

[12] L. Salwinski, C. S. Miller, A. J. Smith, F. K. Pettit, J. U. Bowie, and D. Eisenberg, "The database of interacting proteins: 2004 update," *Nucleic Acids Research*, vol. 32, no. 90001, pp. 449D–451D, 2004.

[13] S. Brohée and J. van Helden, "Evaluation of clustering algorithms for protein-protein interaction networks," *BMC Bioinformatics*, vol. 7, no. 1, p. 488, 2006.

[14] M. He, Y. Wang, and W. Li, "PPI finder: a mining tool for human protein-protein interactions," *PLoS One*, vol. 4, no. 2, Article ID e4554, 2009.

[15] R. McDonald and F. Pereira, "Identifying gene and protein mentions in text using conditional random fields," *BMC Bioinformatics*, vol. 6, no. S1, 2005.